



# **One-Dimensional Simulation of Neutral Helium Transport in Edge Plasmas**

**H.H. Abou-gabal, G.A. Emmert**

**January 1989**

**UWFDM-788**

***FUSION TECHNOLOGY INSTITUTE  
UNIVERSITY OF WISCONSIN  
MADISON WISCONSIN***

### **DISCLAIMER**

This report was prepared as an account of work sponsored by an agency of the United States Government. Neither the United States Government, nor any agency thereof, nor any of their employees, makes any warranty, express or implied, or assumes any legal liability or responsibility for the accuracy, completeness, or usefulness of any information, apparatus, product, or process disclosed, or represents that its use would not infringe privately owned rights. Reference herein to any specific commercial product, process, or service by trade name, trademark, manufacturer, or otherwise, does not necessarily constitute or imply its endorsement, recommendation, or favoring by the United States Government or any agency thereof. The views and opinions of authors expressed herein do not necessarily state or reflect those of the United States Government or any agency thereof.

# **One-Dimensional Simulation of Neutral Helium Transport in Edge Plasmas**

H.H. Abou-gabal, G.A. Emmert

Fusion Technology Institute  
University of Wisconsin  
1500 Engineering Drive  
Madison, WI 53706

<http://fti.neep.wisc.edu>

January 1989

UWFDM-788

**One-Dimensional Simulation of Neutral Helium  
Transport in Edge Plasmas**

**H.H. Abou-gabal and G.A. Emmert**

**Fusion Technology Institute  
Nuclear Engineering and Engineering Physics Department  
University of Wisconsin-Madison  
1500 Johnson Drive  
Madison WI 53706**

**January 1989**

**UWFDM-788**

# One-Dimensional Simulation of Neutral Helium Transport in Edge Plasmas

H. H. Abou-gabal and G.A. Emmert

Nuclear Engineering and Engineering Physics Department

University of Wisconsin-Madison

Madison, Wisconsin 53706

## **Abstract**

A Monte Carlo code for studying the transport of neutral helium atoms near divertor or limiter target plates has been developed. The model is one-dimensional and includes electron impact ionization and elastic scattering by plasma ions. The thermal and streaming motion of the ions along the magnetic field, which can be at an angle to the target plate, is included. The total and differential elastic scattering cross-sections have been calculated classically using an ab initio calculation of the interatomic potential. Results show significant effects of elastic collisions below about 10 eV, causing a substantial fraction of the helium atoms to be reflected back to the target plate. This effect can be beneficial for the pumping of helium from the discharge chamber.

# 1 Introduction

Helium exhaust is an important problem in the design of magnetic fusion reactors.  $\alpha$  particles are produced as a result of the D-T fusion reaction and have to be removed from the system, otherwise the burning fuel will be diluted and the fusion reactivity will be decreased.  $\alpha$  particles recombine on a divertor plate or a limiter target and form neutral helium atoms.

Helium atoms generally have a longer mean free path than the neutral hydrogenic species, and therefore penetrate further into the main plasma. This effect can cause helium de-enrichment and make the pumping of helium gas a harder task. As an example, consider Fig. 1 which shows a divertor configuration proposed previously for use in the TIBER-II tokamak. Hydrogenic ions ( $D^+$  and  $T^+$ ) as well as  $\alpha$  particles following the magnetic field lines in the scrape-off layer hit the divertor plate and get neutralized. If the striking point is inside one of the holes along the plate, the resulting neutral particle is scattered outside the system and can be driven to the pump duct as shown in Fig. 1-b (particle a), otherwise the particle gets scattered towards the plasma (particle b). In the case of hydrogenic species, due to the charge exchange process between the ion and the neutral particle, the latter can return back to the divertor plate where it has a chance to go through one of the holes and into the pump duct. A critical issue for this target plate concept is the pumping of helium. For helium, since we are treating a low temperature regime (below about 40 eV), the proton-helium charge exchange reaction can be neglected as compared to electron impact ionization and, although charge exchange of helium with  $He^+$  and  $He^{2+}$  ions is considerable in the low temperature range, the low density of these ions, as compared to the main plasma density, makes this reaction negligible. Therefore, considering these interactions only, neutral helium has little chance to be backscattered towards the plate

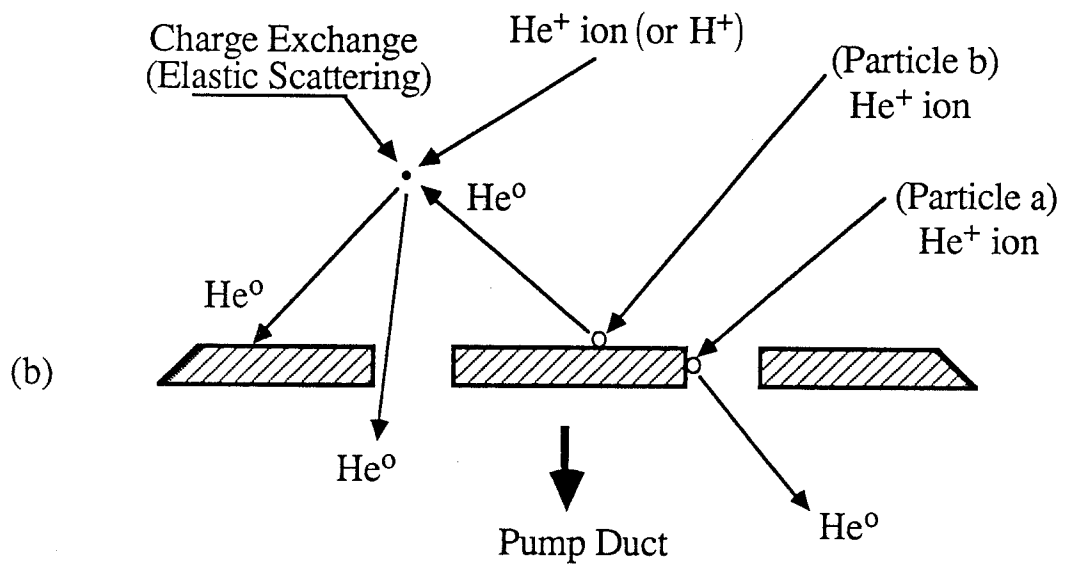
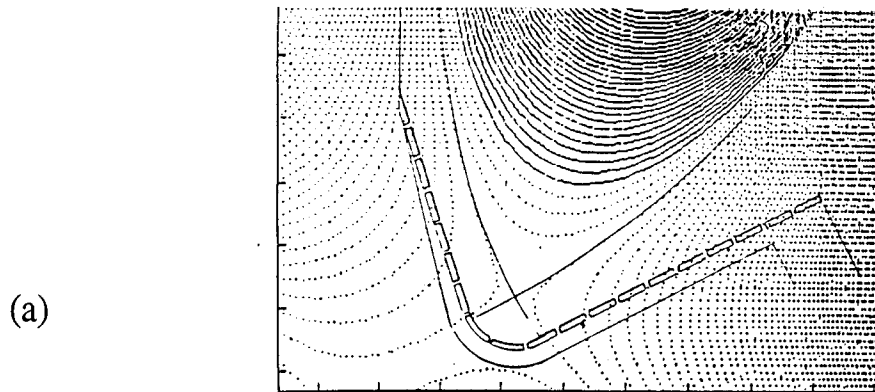


Figure 1: (a) TIBER-II's previously proposed divertor with its flat vented plates (from LLNL/TIBER 86-25). (b) Recycling at the plate.

unless it gets ionized and returns in the form of an ion. Another interaction which may cause backscattering of the neutral helium to the divertor plate is the elastic scattering of neutral helium by hydrogenic ions. If sufficient backscattering of helium atoms to the plate can be obtained, then pumping of the helium from the system can be accomplished.

Potters and Goedheer [1,2] were the only ones to consider the elastic scattering process when treating the problem of neutral helium transport in plasma. Their work is based on a numerical solution of the Boltzmann equation and is restricted to only one-dimensional problems. Since the solution of the Boltzmann equation using the exact form of the elastic collision operator is a rather difficult task, they considered this problem using a simple model (BGK model) in which collisions cause the neutral helium distribution function to relax towards the Maxwellian distribution function at the local temperature, with a relaxation time  $\tau_{He}$  assumed to be independent of velocity. In other works [3,4,5,6], the Monte Carlo method has been used to study helium atom transport, but the process of elastic scattering with ions has not been considered.

In this report, we consider helium transport in the low temperature plasma edge region. We assume that the neutral helium undergoes either electron impact ionization or elastic scattering on the background ions. A one-dimensional transport code, 1DHET, based on Monte Carlo techniques, has been written to simulate helium atom transport. This allows us to consider the elastic scattering process in a more accurate way and to include the finite flow velocity of the ions with which the helium is colliding. The 1DHET code treats only one-dimensional problems but the use of the Monte Carlo method makes possible its extension to two-dimensional cases.

In the next section, cross sections for the reactions considered between the helium atoms and the plasma are presented. Section 3 contains the model for wall reflection, while a description of the Monte Carlo simulation is given in section 4. Finally, in section 5,



numerical applications of the code 1DHET and the discussion of the results obtained are included.

## 2 Plasma-Neutral Helium Interactions

The electron impact ionization rate coefficients for helium are obtained from the formulation of Bell *et al.* [7]. The rate coefficients  $\langle \sigma \cdot v \rangle_e$  (cross section at a given energy multiplied by electron velocity  $v$  at the same energy, and averaged over a Maxwellian velocity distribution of the electrons) are plotted in Fig. 2.

Because of the lack of data on the elastic scattering of neutral helium by hydrogenic ions, we calculated the needed cross sections using a classical model. Assume a spherically symmetric potential,  $V(r)$ , with a long range attraction, an attractive well and a short-range repulsion. From elementary considerations of energy and momentum conservation one obtains [8,9,10] an explicit expression for the classical deflection function,  $\chi$ ,

$$\chi(b, g) = \pi - 2b \int_{r_m}^{\infty} \frac{dr}{r^2 \sqrt{1 - \frac{V(r)}{\frac{1}{2}\mu g^2} - \left(\frac{b}{r}\right)^2}}, \quad (1)$$

where  $b$  is the impact parameter,  $\mu$  is the reduced mass,  $g$  is the initial relative speed of the colliding particles and  $r_m$ , the distance of closest approach in the encounter, is the outermost zero of

$$1 - \frac{V(r_m)}{\frac{1}{2}\mu g^2} - \left(\frac{b}{r_m}\right)^2 = 0.$$

The deflection function  $\chi$  is positive for net repulsive and negative for net attractive trajectories. The observable scattering angle in the center of mass system is

$$\Theta = |\chi| \quad \text{with} \quad 0 \leq \Theta \leq \pi.$$

Let  $\sigma(\Theta, E)$  be the differential elastic scattering cross section where  $E$  is the center of mass energy,  $E = \frac{1}{2}\mu g^2$ .  $\sigma(\Theta, E)$  is expressible directly in terms of the deflection function

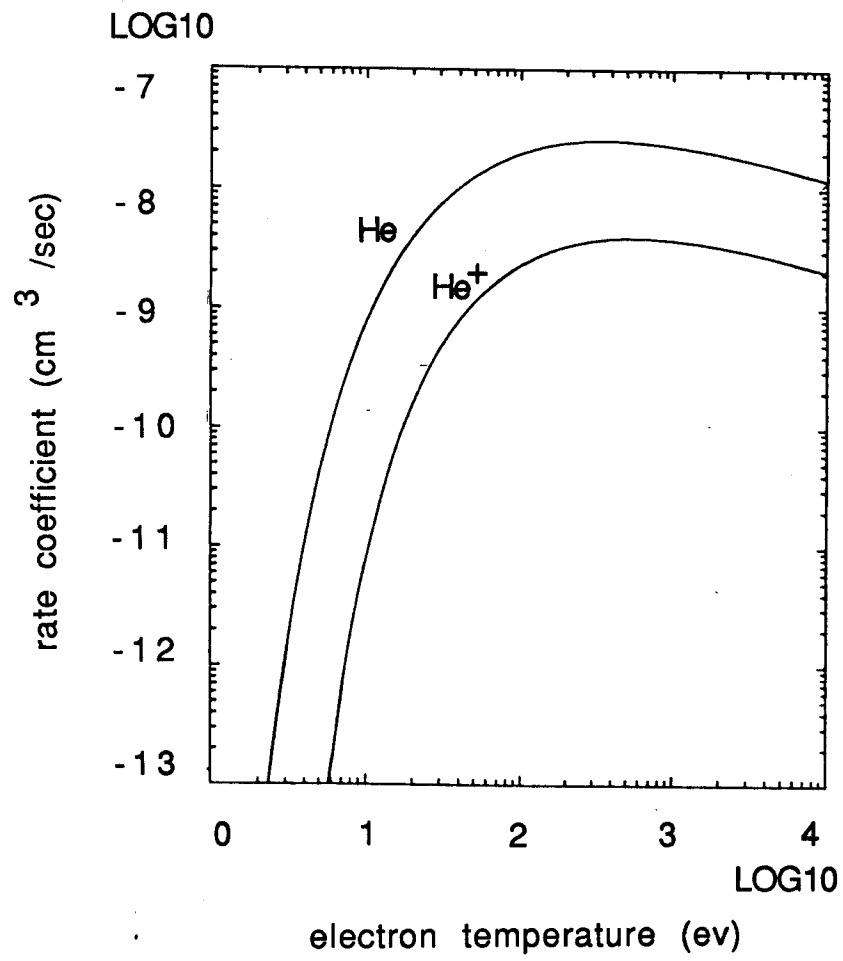


Figure 2: Electron impact ionization rate coefficients for helium[7].

by the relation

$$\sigma(\Theta, E) = \sum_i \frac{b_i}{\sin \Theta} \left| \frac{db}{d\chi} \right|_i, \quad (2)$$

where the summation is over the various values of  $b$  giving rise to the same value of  $\Theta$ .

The total elastic scattering cross section,  $\sigma_s$ , is defined as

$$\sigma_s(E) = 2\pi \int_0^\infty \sigma(\Theta, E) \sin \Theta d\Theta. \quad (3)$$

For the form of  $V(r)$ , we utilize the results of ab initio calculations by Wolniewicz [11] in which he calculated adiabatic values for the intermolecular potential of the molecular ion  $\text{HeH}^+$ . Helbig, Millis and Todd [12] have fit these calculations to the following analytical function

$$V(r) = \frac{2}{r} e^{-\frac{r}{A}} \left[ 1 + \frac{r}{A} + \frac{1}{2} r^2 \left( \frac{1}{A^2} - \frac{U}{B} \right) \right] - \frac{U}{\left[ 1 + \frac{r}{B} + \left( \frac{r}{C} \right)^2 + \frac{2Ur^4}{\alpha} \right]},$$

where  $U$ , the difference between the ground-state energies of He and  $\text{Li}^+$ , equals 4.37311 hartrees (1 hartree = 27.2097 eV),  $\alpha$ , the polarizability of He, equals 1.3835 bohr (1 bohr =  $0.52917 \times 10^{-8}$  cm),  $A = 0.442$ ,  $B = 0.505$ , and  $C = 0.451$ .

This form of  $V(r)$  is plotted in Fig. 3. Differential elastic scattering cross sections at different values of  $E$  have been calculated and some of them have been compared to the results of Helbig *et al.* [12]. In Fig. 4, the classical deflection function is plotted versus the impact parameter for  $E = 5.79567$  eV. Fig. 5 shows the corresponding classical differential elastic scattering cross section versus  $\Theta$ . As shown in the figure, our curve is in good agreement with the Helbig *et al.* results. The total elastic scattering cross section is presented in Fig. 6 versus the helium kinetic energy in a frame with the proton at rest and in Fig. 7 versus the helium-proton relative speed,  $g$ .

The elastic scattering rate coefficient  $\langle \sigma \cdot v \rangle_s$  is given by

$$\langle \sigma \cdot v \rangle_s = \int \sigma_s(g) |\bar{v}_p - \bar{V}| f_i(\bar{V}) d\bar{V}, \quad (4)$$

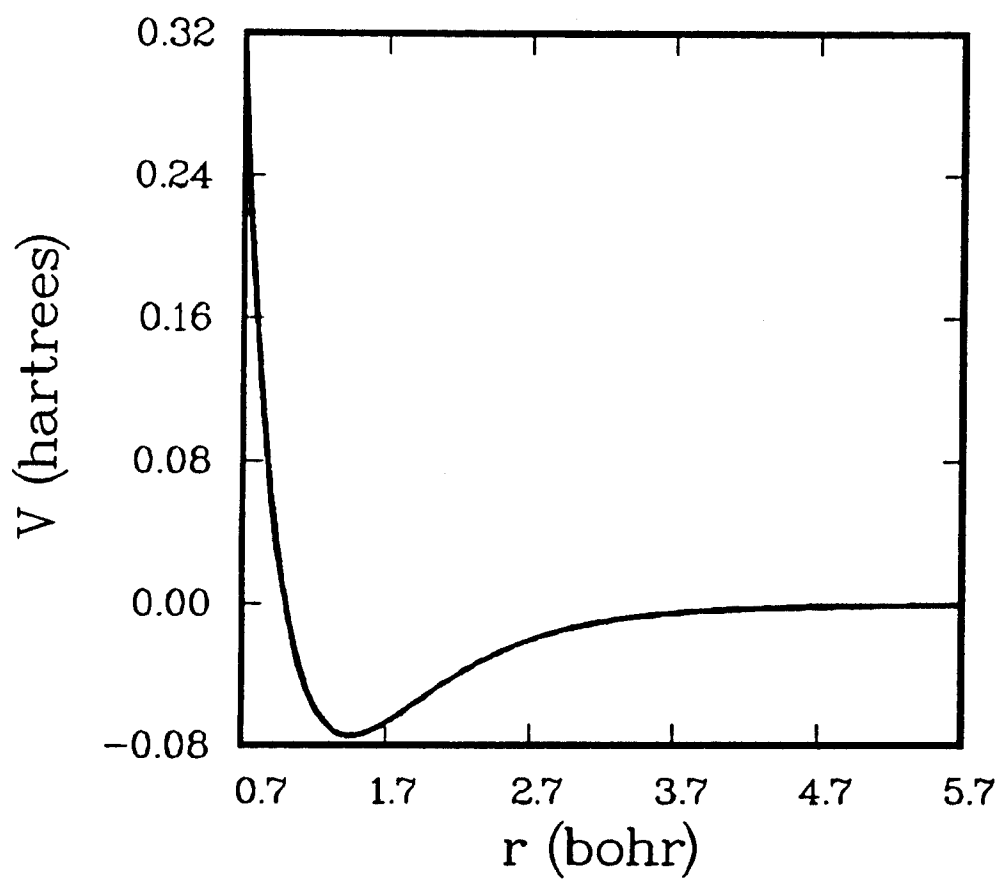


Figure 3: Wolniewicz potential versus proton-helium atom separation distance.

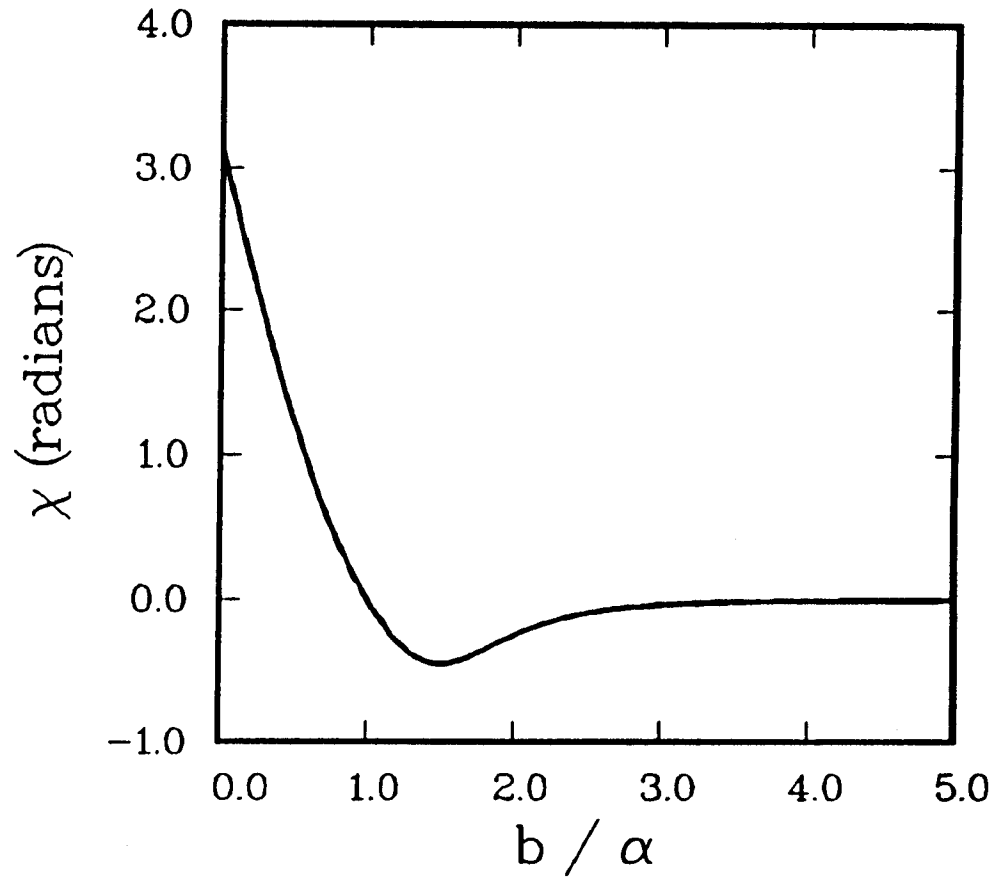


Figure 4: Classical deflection function versus normalized impact parameter (center of mass energy = 5.79567 eV).

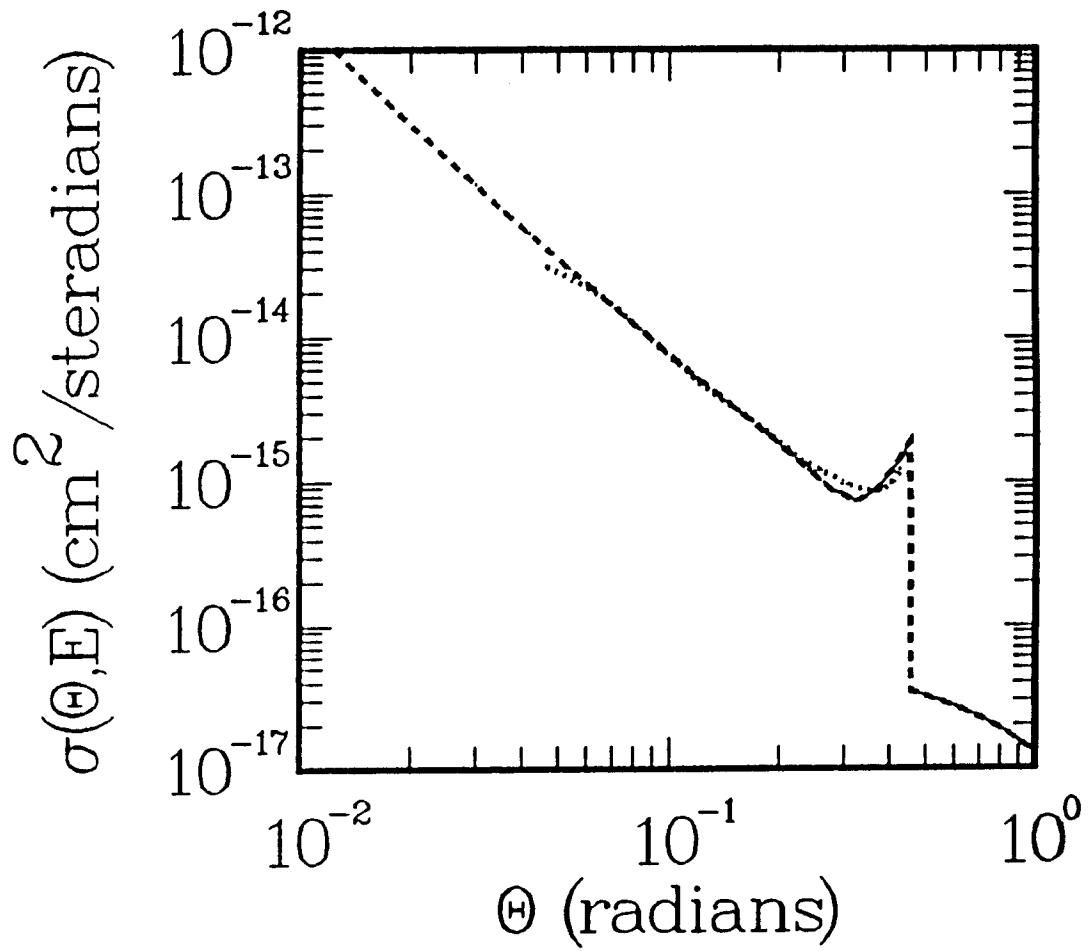


Figure 5: Classical differential elastic scattering cross section (center of mass energy = 5.79567 eV), - - - our results, ... Helbig results.

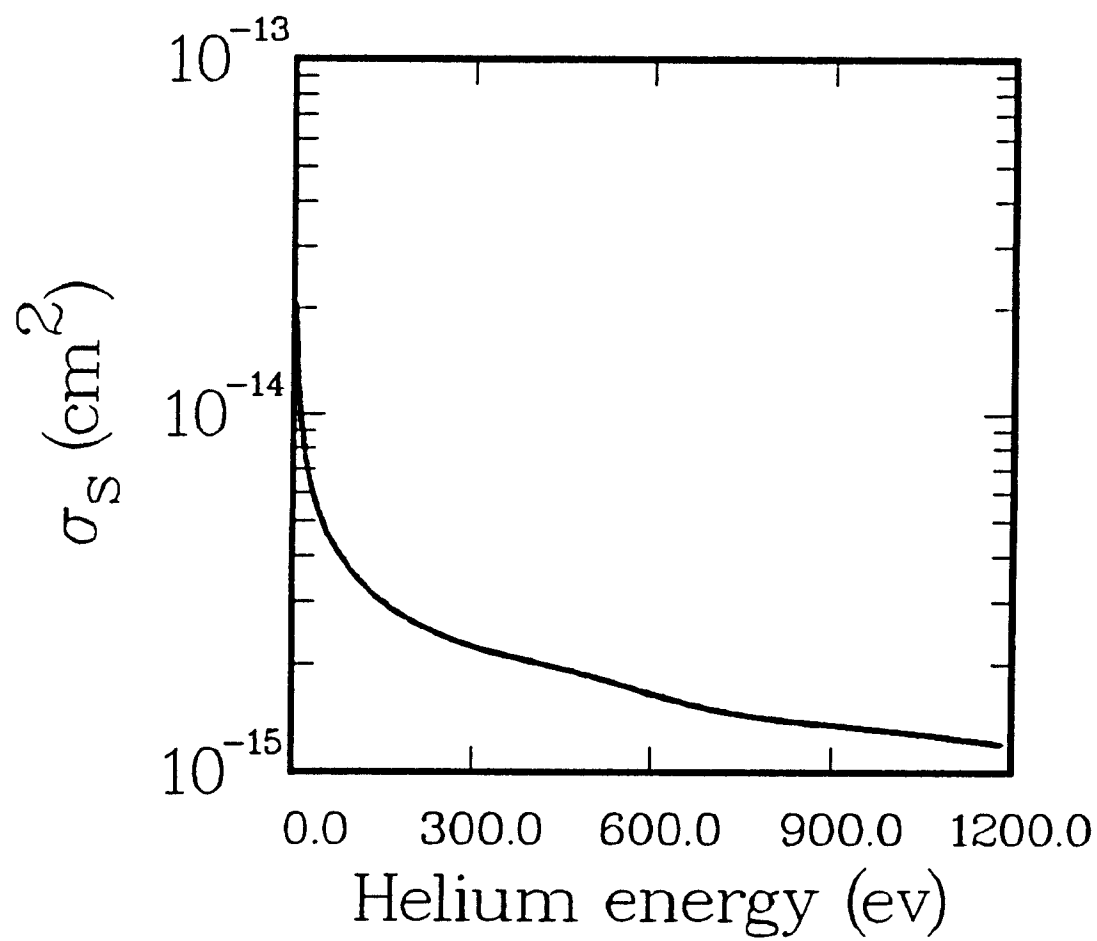


Figure 6: Total elastic scattering cross section versus helium kinetic energy.

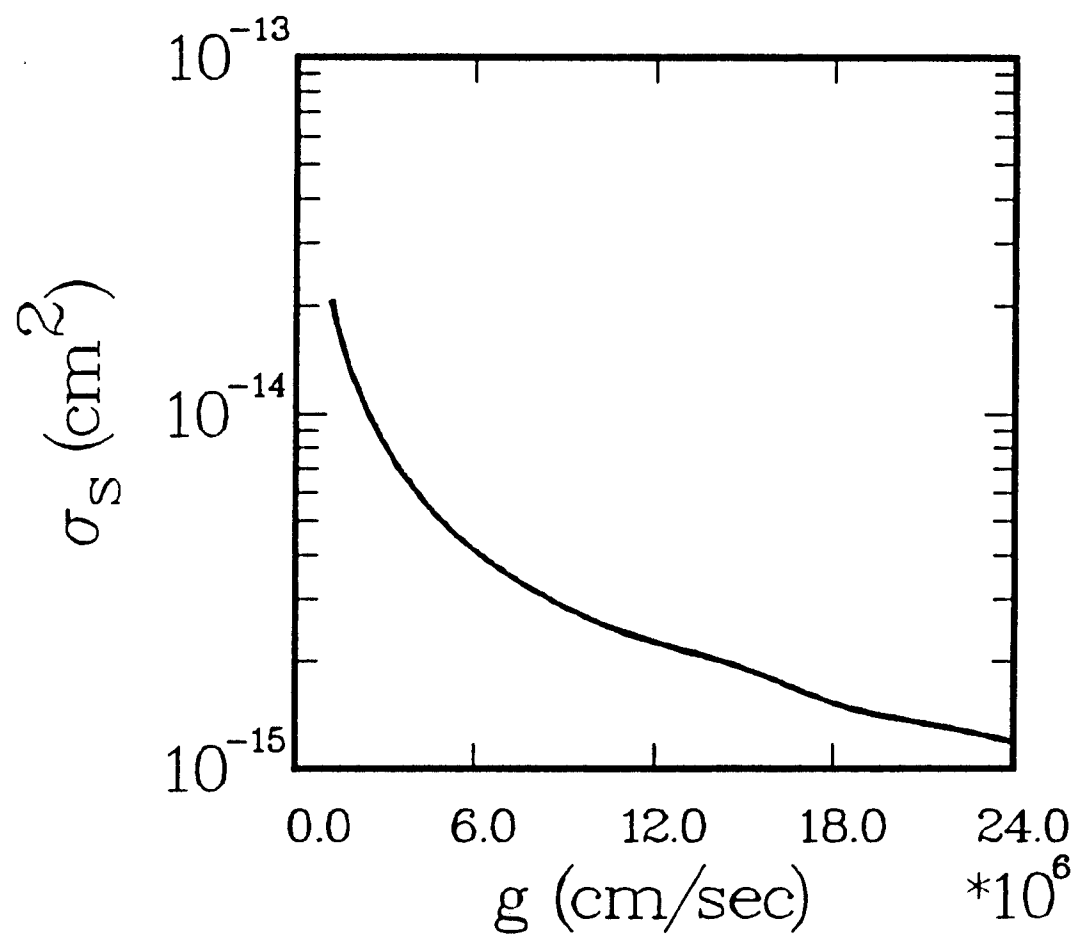


Figure 7: Total elastic scattering cross section versus helium-proton relative speed.



where  $\sigma_s(g)$  is the elastic scattering cross section as a function of the relative speed  $g$ ,  $g = |\bar{v}_p - \bar{V}|$ ,  $\bar{v}_p$  is the velocity of the neutral helium particle,  $\bar{V}$  is the ion velocity and  $f_i(\bar{V})$  is the ion distribution function.

Since numerical integration of Eq. (4) at each flight of the tracked particle is out of the question, an approximate solution has been introduced [4]. The relative speed  $g$  has been substituted with an average speed  $g^*$  which is in some way representative of the velocity population. In particular, to simplify the calculations, let

$$g^* = \langle g^2 \rangle^{1/2},$$

with

$$\langle g^2 \rangle = \int g^2 f_i(\bar{V}) d\bar{V}.$$

For  $f_i(\bar{V})$  equal to a shifted Maxwellian,

$$f_i(\bar{V}) = \left( \frac{m_H}{2\pi k T_i} \right)^{1/2} \exp \left[ -\frac{m_H}{2k T_i} (\bar{V} - \bar{a})^2 \right], \quad (5)$$

where  $m_H$  is the mass of the hydrogenic ion,  $T_i$  and  $\bar{a}$  are the ion temperature and the ion flow velocity respectively, we have [4]

$$g^* = \left[ \frac{3k T_i}{m_H} + |\bar{a} - \bar{v}_p|^2 \right]^{1/2}.$$

Eq. (4) is then written as

$$\langle \sigma \cdot v \rangle_s = \sigma_s(g^*) g^*.$$

### 3 Wall Interactions

In this section, the modelling of the interactions of ions and neutrals with divertor or limiter target plates will be described. In a steady state condition, plasma ions hitting a

wall or a plate are neutralized and return back to the plasma as a result of mainly two processes: backscattering and re-emission.

Particles of energy  $E_0$  bombarding a surface of a solid at an angle of incidence,  $\alpha$ , relative to the surface normal, penetrate for a short distance into the solid and are backscattered (predominantly) as neutrals to the surface with a probability  $R_N$ , which is a function of  $E_0$  and  $\alpha$ .  $R_N$  is called the particle reflection coefficient and defined as the average number of particles backscattered per incident particle. The reflected energy is expressed as a fraction  $R_E(E_0, \alpha)$  of the incident energy. The coefficient  $R_E$  is called the energy reflection coefficient. Therefore, the mean energy of the backscattered particles  $\bar{E}(E_0, \alpha)$  is a result of these definitions

$$\bar{E}(E_0, \alpha) = E_0 \frac{R_E(E_0, \alpha)}{R_N(E_0, \alpha)}. \quad (6)$$

Particle and energy reflection coefficients depend further on the solid material and the incident particle.

In many publications, backscattering data are represented not as a function of the incident energy but as a function of the reduced energy,  $\varepsilon$ , introduced by Lindhard *et al.* [13] and given by

$$\varepsilon = 32.55 \left( \frac{m_1}{m_1 + m_2} \right) \frac{1}{Z_1 Z_2 (Z_1^{2/3} + Z_2^{2/3})^{1/2}} E_0,$$

with  $E_0$  in keV and  $m_1, Z_1, m_2, Z_2$  being the mass and nuclear charge of the incident particles and target atoms. The use of  $\varepsilon$  instead of the actual energy  $E_0$  allows one to scale approximately the backscattering data for different ion-target combinations as long as  $m_2 \gg m_1$ .

In our model, we adopted the forms of the reflection coefficients used by Cupini *et*

al. [4]. These are given by

$$R_N(\varepsilon) = \begin{cases} 1 & \varepsilon \leq 3 \times 10^{-4} \\ 0.1885 - 0.2265 \log_{10} \varepsilon & 3 \times 10^{-4} < \varepsilon \leq 7 \\ 0 & \varepsilon > 7 \end{cases}$$

$$R_E(\varepsilon) = \begin{cases} 1 & \varepsilon \leq 2 \times 10^{-4} \\ -0.25 \log_{10} \varepsilon & 2 \times 10^{-4} < \varepsilon \leq 0.1 \\ 0.07 - 0.18 \log_{10} \varepsilon & 0.1 < \varepsilon \leq 2 \\ 0 & \varepsilon > 2 \end{cases}$$

For hydrogen and helium bombardment of Fe, Ni and stainless steel, the following formulas have been adopted:

$$R_N(\varepsilon) = [(1 + 3.2116\varepsilon^{0.34334})^{3/2} + (1.3288\varepsilon^{3/2})^{3/2}]^{-2/3},$$

$$R_E(\varepsilon) = [(1 + 7.1172\varepsilon^{0.35250})^{3/2} + (5.2757\varepsilon^{3/2})^{3/2}]^{-2/3}.$$

For helium incident on graphite walls, the following expressions have been used

$$R_N(E_o) = \begin{cases} 0.459 E_o^{-0.3} & E_o \leq 1000 \\ 274 E_o^{-1.22} & E_o > 1000 \end{cases}$$

$$R_E(E_o) = \begin{cases} 0.313 E_o^{-0.417} & E_o \leq 1000 \\ 473 E_o^{-1.476} & E_o > 1000 \end{cases}$$

The coefficient  $R_N$  increases with the angle of incidence,  $\alpha$ , and approaches 1 for grazing incidence. To account for this, the following formula has been used

$$R_N(E_o, \alpha) = [R_N(E_o) - 1] \cos \alpha + 1,$$

where  $R_N(E_o, \alpha)$  is the particle reflection coefficient for non-normal incidence, and  $R_N(E_o)$  is the particle reflection coefficient for normal incidence.

Since there is a lack of agreement between theoretical and experimental data for the dependence of the energy reflection coefficient on the incidence angle [14,15], any dependence of  $R_E$  on  $\alpha$  has been neglected in our model.

Therefore, when a particle history reaches a wall the event of backscattering is chosen with probability  $R_N$  and the energy of the reflected particle is determined from Eq. (6). As for the angle of the emerging particle, its distribution is reasonably approximated by a cosine law [14], together with a uniformly distributed azimuthal angle. Particles which are not backscattered, slow down to thermal energies and are re-emitted with a speed chosen from a speed Maxwellian distribution

$$f(v) = 4\pi \left( \frac{m_{He}}{2\pi k T_w} \right)^{3/2} v^2 \exp \left[ -\frac{m_{He}}{2k T_w} v^2 \right], \quad (7)$$

where  $T_w$  is the wall temperature and  $k$  is the Boltzmann constant. The angles of the re-emitted particle are chosen as in the case of backscattering.

## 4 Monte Carlo Simulation

The geometry of the problem considered and the coordinates used are shown in Fig. 8. The region of interest has a maximum width of  $Z_{max}$  and is divided into zones of uniform plasma parameters. The plasma parameters, such as the electron temperature,  $T_e$ , the ion temperature,  $T_i$ , the plasma density,  $n_p$ , the ion flow velocity,  $\bar{a}$ , and the sheath and pre-sheath potential,  $\Phi$ , are kept constant during the Monte Carlo calculation.

### 4.1 Sampling of the Neutral Source Particle

The code allows the performance of two distinct calculations:

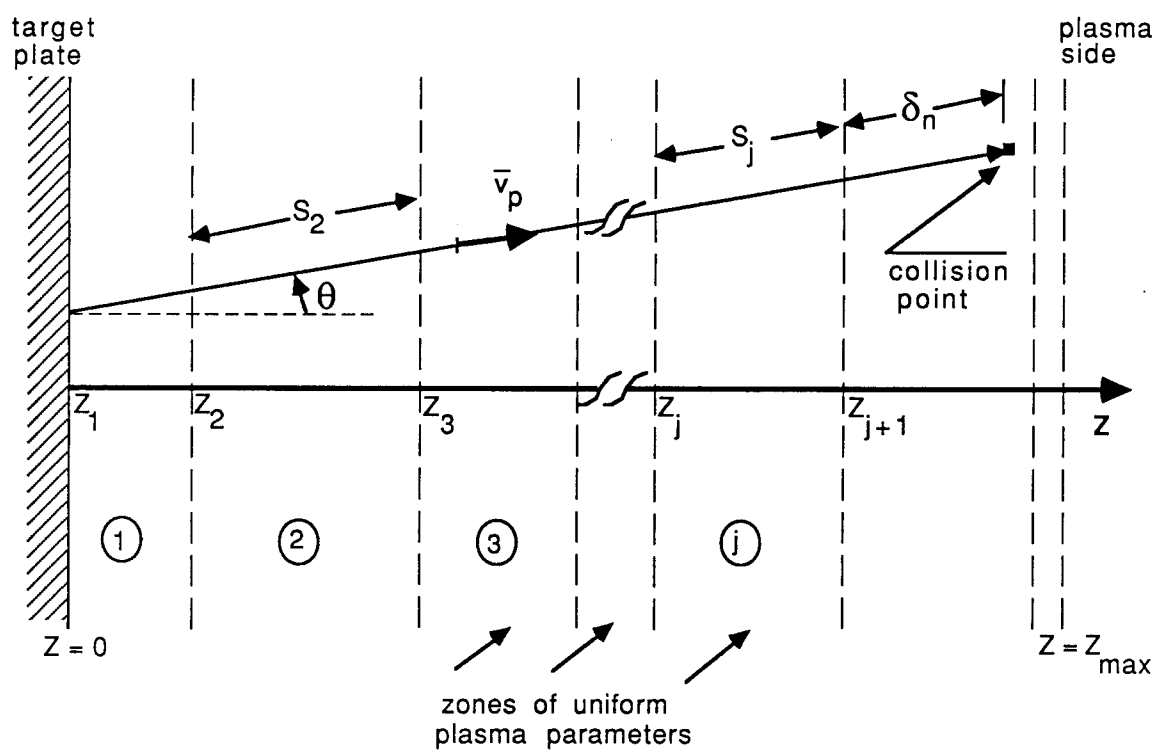


Figure 8: Geometry and coordinates.

- The first calculation assumes a monoenergetic source of neutral helium particles placed at the target plate. It also assumes that the reflection at the plate is neglected, *i.e.*, when a helium atom leaving the plasma strikes the plate, it will be considered lost from the system. This calculation allows us to obtain the probability for a helium atom born at the target plate to be scattered by the plasma back to the plate because of elastic scattering with plasma ions.
- In the second calculation, the neutral helium source is due to the neutralization of the helium ions incident on the plate. These ions get reflected as neutral helium, as described in section 3. In this case the reflection at the plate is taken into account, *i.e.*, helium atoms striking the plate are allowed either to get reflected back as in section 3 or to escape from the system.

For the second type of calculation, the neutral source particle has its energy obtained as follows:

- An  $\alpha$  particle incident on the target plate has its velocity,  $\bar{v}_i$ , chosen from a shifted Maxwellian distribution

$$f(\bar{v}_i) = \left( \frac{m_{He}}{2\pi k T_{i1}} \right)^{1/2} \exp \left[ - \frac{m_{He}}{2k T_{i1}} (\bar{v}_i - \bar{a}_1)^2 \right],$$

where  $T_{i1}$  is the edge ion temperature and  $\bar{a}_1$  is the edge ion flow velocity.

- Because the  $\alpha$  particle is accelerated through the sheath and pre-sheath potential,  $\Phi$ , it will therefore have a total incident energy  $E_o$  given by

$$E_o = \frac{1}{2} m_{He} v_i^2 + 2\Phi,$$

and it is assumed to be incident normal to the plate.

- Using the reflection model described in section 3, the reflected helium atom will have its velocity  $\bar{v}_p$  specified.

## 4.2 Sampling of the Collision

The path length estimator technique [16,17] is used to track the helium particle until a collision point is obtained. As mentioned before, at the collision point the neutral helium atom can either be ionized by electrons or elastically scattered by background ions. Ionization is sampled by using the method of suppression of absorption [4,5,17].

The elastic scattering is treated as follows:

1. The target ion has its velocity,  $\bar{V}$ , sampled from a shifted Maxwellian distribution given by Eq.(5).
2. Since the collision problem is more easily treated when one particle is at rest, we transform our problem to the frame where the target ion is at rest. In this frame, frame no. 2, the helium atom will have a velocity  $\bar{v}_r$  given by

$$\bar{v}_r = \bar{v}_p - \bar{V},$$

and an energy obtained as

$$E_r = \frac{1}{2} m_{He} v_r^2.$$

3. A transformation to a center of mass (COM) frame is then performed with the velocity of the center of mass obtained as  $\bar{v}_{CM} = \frac{m_{He}\bar{v}_r}{m_{He}+m_H}$ .
4. Since the scattering is anisotropic, the scattering angle in the COM frame,  $\Theta$ , will be sampled using a method employed in the transport of neutrons [18]. This method can be devised by tabulating, for specific incident energies, the  $(n+1)$  center-of-mass

angles that correspond to  $n$  equally probable intervals of the cumulative distribution function,  $P_i$ , where  $P_i$  is given by

$$P_i = 2\pi \int_{-1}^{(\cos \Theta)_i} \frac{\sigma(\Theta, E_r)}{\sigma_s(E_r)} d(\cos \Theta) \quad i = 0, 1, 2, \dots, n.$$

Here  $n$  is the number of equally likely intervals, set equal to 32 in our calculation,  $\sigma(\Theta, E_r)$  is the differential elastic scattering cross section and  $\sigma_s(E_r)$  is the total elastic scattering cross section. Our model contains such tables for 30 values of the incident energy  $E_r$ . The scattering angle,  $\Theta$ , is then determined by linear interpolation between consecutive tables.

5. The scattering angle in frame no. 2,  $\theta_2$ , is then found from

$$\cos \theta_2 = \frac{1 + A \cos \Theta}{(1 + 2A \cos \Theta + A^2)^{1/2}},$$

where  $A = m_H/m_{He}$ . The speed of the emerging helium atom in frame no. 2,  $v'_r$ , can be calculated using

$$v'_r = v_r \frac{(1 + A^2 + 2A \cos \Theta)^{1/2}}{1 + A}.$$

The direction cosines of the emerging helium atom in frame no. 2 result from the following equations [19]

$$\text{if } |\omega_{rz}| < 0.999999,$$

$$\begin{aligned} \omega'_{rx} &= \frac{\sin \theta_2}{\sqrt{1 - \omega_{rz}^2}} [\omega_{rx} \omega_{rz} \cos \varphi - \omega_{ry} d] + \omega_{rx} \cos \theta_2, \\ \omega'_{ry} &= \frac{\sin \theta_2}{\sqrt{1 - \omega_{rz}^2}} [\omega_{ry} \omega_{rz} \cos \varphi + \omega_{rx} d] + \omega_{ry} \cos \theta_2, \\ \omega'_{rz} &= -\sqrt{1 - \omega_{rz}^2} \sin \theta_2 \cos \varphi + \cos \theta_2 \omega_{rz}. \end{aligned}$$

Otherwise,

$$\omega'_{rx} = \sin \theta_2 \cos \varphi,$$



$$\begin{aligned}\omega'_{ry} &= d \sin \theta_2, \\ \omega'_{rz} &= \omega_{rz} \cos \theta_2.\end{aligned}$$

The azimuthal angle  $\varphi$  is sampled isotropically from

$$\varphi = \pi(2\xi - 1),$$

where  $\xi$  is a random number uniformly distributed between 0 and 1.  $d$  is given by

$$d = \begin{cases} -\sin \varphi & \varphi < 0 \\ \sin \varphi & \varphi \geq 0. \end{cases}$$

6. Transforming back to our initial frame, we have the velocity of the scattered helium atom as

$$\begin{aligned}\overline{v'_p} &= \overline{v'_r} + \overline{V}, \\ &= (v'_r \omega'_{rx} + V_x) \hat{x} + (v'_r \omega'_{ry} + V_y) \hat{y} + (v'_r \omega'_{rz} + V_z) \hat{z},\end{aligned}$$

which can be written as

$$\overline{v'_p} = v'_{px} \hat{x} + v'_{py} \hat{y} + v'_{pz} \hat{z},$$

from which, the speed and the direction cosines of the scattered helium atom are calculated by

$$\begin{aligned}v'_p &= (v'^2_{px} + v'^2_{py} + v'^2_{pz})^{1/2}, \\ \omega'_x &= \left[ 1 - \left( \frac{v'_{pz}}{v'_p} \right)^2 \right]^{1/2} \frac{v'_{px}}{[v'^2_{px} + v'^2_{py}]^{1/2}}, \\ \omega'_y &= \left[ 1 - \left( \frac{v'_{pz}}{v'_p} \right)^2 \right]^{1/2} \frac{v'_{py}}{[v'^2_{px} + v'^2_{py}]^{1/2}}, \\ \omega'_z &= \frac{v'_{pz}}{v'_p}.\end{aligned}$$

The scattered helium atom is then tracked until the particle either escapes from the system or is ionized. A new particle is then launched at the plate and all the above steps are repeated again.

## 5 Results

The 1DHET code allows the calculation of the neutral helium density distribution and the helium current outgoing to the plate, which gives the number of helium particles scattered back to the plate. One can also obtain the helium current escaping to the plasma side, the number of helium particles escaping at the plate to the pump duct as well as the energy spectrum of the neutral helium at the plate.

A parametric study has been performed to examine the dependence of the helium current outgoing to the plate on the ion temperature and on the ion flow velocity. We assume a hydrogen plasma with uniform and equal electron and ion temperatures in a region of maximum width  $Z_{max} = 7$  cm. The plasma has a uniform density set equal to  $1 \times 10^{14} \text{ cm}^{-3}$ . Ions and electrons follow magnetic field lines which are at an angle of  $10^\circ$  to the target plate, which is taken to be iron. The sheath and pre-sheath potential,  $\Phi$ , is assumed to be equal to  $3T_e$ .

Two different calculations have been done. The first considers only the emission of 0.05 eV atoms at the plate and their reflection by elastic scattering with the ions. The second calculation considers helium ions incident on the plate, their backscattering and re-emission as atoms, and also backscattering or re-emission when helium atoms strike the plate.

In the first case the atoms are emitted with an energy of 0.05 eV at the target plate. Fig. 9 shows the neutral helium current scattered by the plasma back to the plate versus

the plasma temperature. Since this current is normalized to 1 source particle/cm<sup>2</sup> s, it represents the probability that a 0.05 eV atom born at the plate will be elastically scattered by the ions back to the plate. As shown in Fig. 9, this probability increases as the ion temperature decreases and becomes significant below 10 eV. The low reflection probability of the plasma above 10 eV is because electron impact ionization rises rapidly with electron temperature and becomes dominant above 10 eV.

The second calculation is for neutral helium atoms resulting from the neutralization and reflection of  $\alpha$  particles incident on the plate. Fig. 10 shows the helium atom current reflected by the plasma by elastic scattering with ions versus the ion temperature. As can be seen, the helium current follows the same behavior as in the first case, but the helium current is somewhat lower in this case. This is because most of the neutral atoms arising from the neutralization of  $\alpha$  particles are more energetic than the 0.05 eV atoms considered in the first case. These energetic particles penetrate further into the plasma before being scattered or ionized. Those atoms which are scattered back toward the plate by elastic scattering with ions have a greater probability of being ionized before returning to the plate. Fig. 11 shows the dependence of the outgoing helium current on the ion flow speed for a plasma temperature equal to 6 eV. As can be seen, the probability of an ion returning to the plate is only weakly dependent on the ion flow speed. Hence the flow of the ions toward the plate is not an important effect in these results.

## 6 Conclusion

Transport of neutral helium in the low temperature region near divertor or limiter target plates has been studied using Monte Carlo techniques. Two different calculations have been done. The first considers helium atoms born from a monoenergetic source placed at

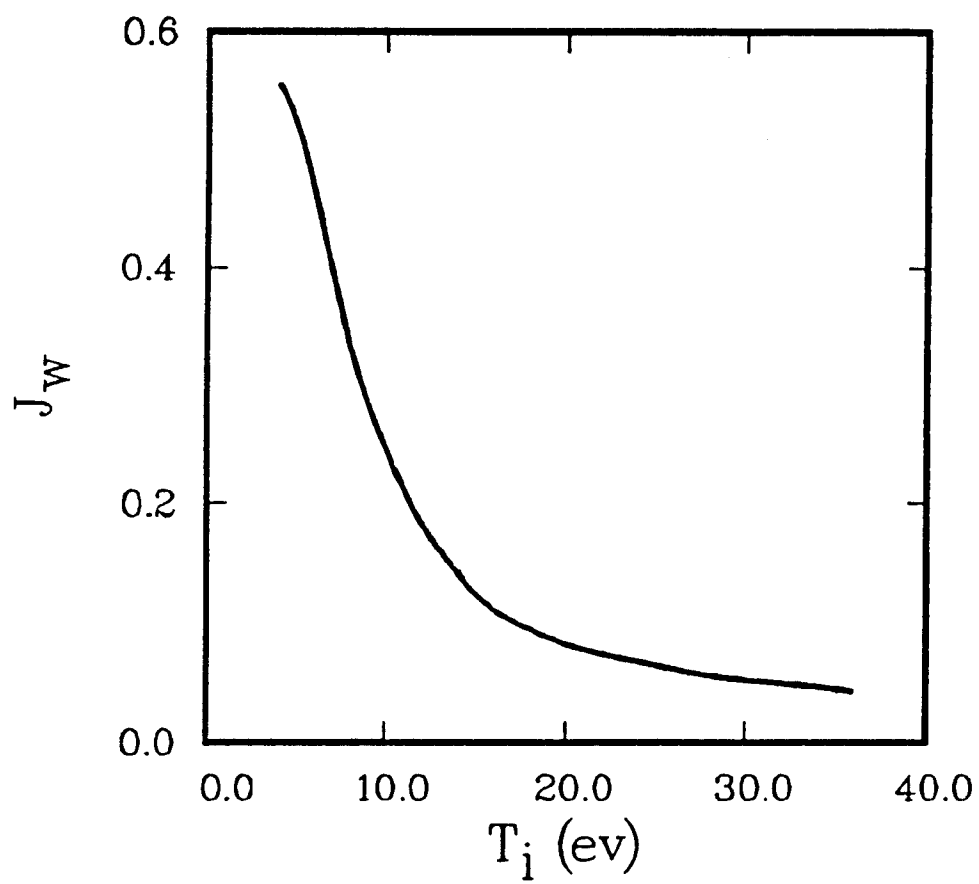


Figure 9: Neutral helium current to the plate versus temperature.

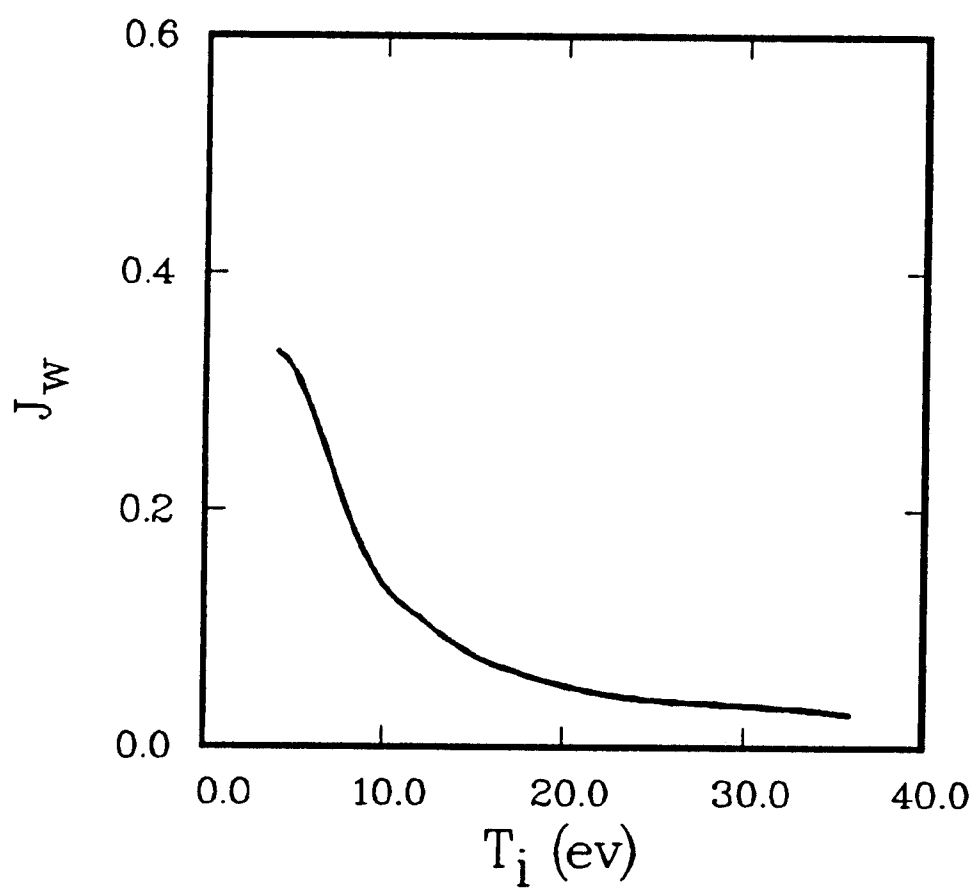


Figure 10: Neutral helium current to the plate versus temperature.

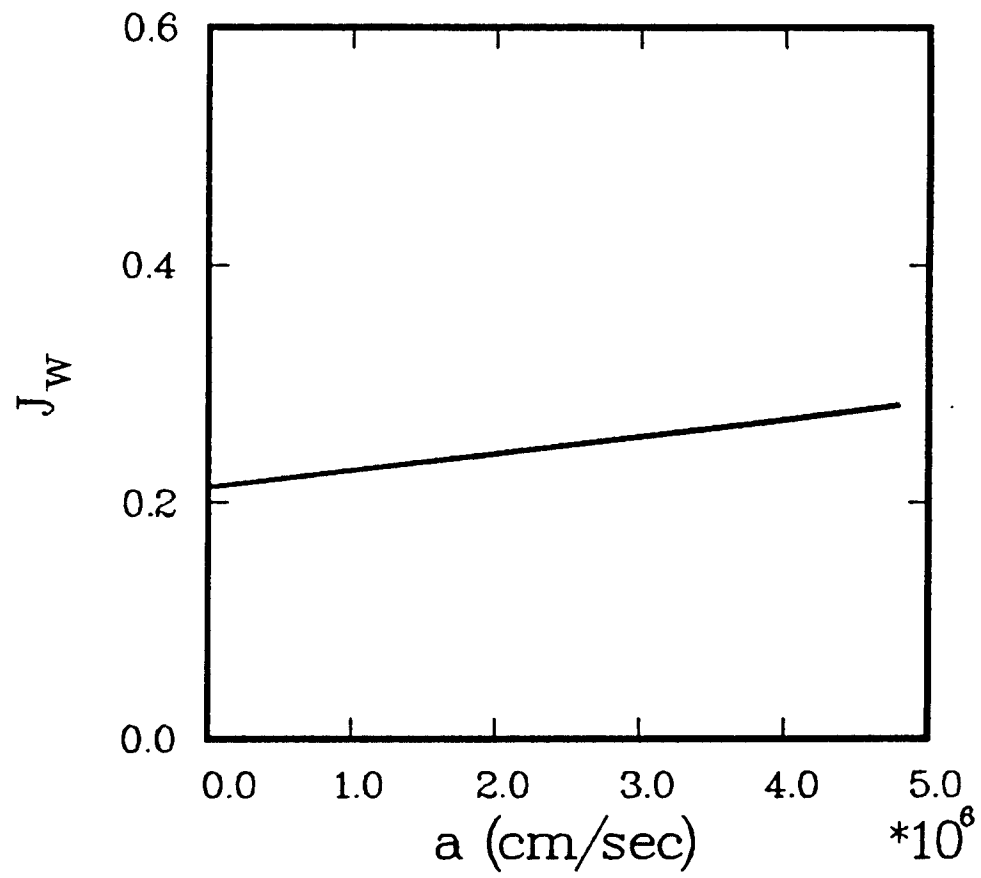


Figure 11: Neutral helium current to the plate versus ion flow speed.

### **Acknowledgement**

This research was supported by the Department of Energy under contract DE-FG02-86ER53218.